Available online at www.sciencedirect.com
ScienceDirect
International Journal of Thermal Sciences 47 (2008) 972–984
International Journal of Thermal Sciences
www.elsevier.com/locate/ijts

Unsteady conjugate forced convection heat/mass transfer from a finite flat plate

Gh. Juncu *

Politehnica University Bucharest, Catedra Inginerie Chimica, Polizu 1, 78126 Bucharest, Romania

Received 24 March 2007; received in revised form 6 September 2007; accepted 6 September 2007
Available online 10 October 2007

Abstract

Numerical methods are used to investigate the transient, conjugate, forced convection heat/mass transfer from a finite flat plate to a steady stream of viscous, incompressible fluid. The heat/mass balance equations were solved numerically in Cartesian coordinates by a finite difference method. The values considered for the plate Reynolds number and Prandtl number are $Re = 100$ and $Pr = 0.1$, 1 and 10. The computations were focused on the influence of the physical properties ratios and aspect ratio on the heat/mass transfer rate.

Keywords: Conjugate heat/mass transfer; Forced convection; Finite plate; Laminar flow; Finite difference method

1. Introduction

The finite/infinite flat plate, the infinite cylinder and the sphere are the benchmark problems for the analysis of heat/mass transfer in external flows. The phrase "conjugate heat transfer" was used for the first time in [1] to describe the heat transfer between an internally heated semi-infinite flat plate and a fluid in laminar flow. Perelman [1] analysed the coupling of forced convective heat transfer in a boundary layer flow over a flat plate of finite thickness with two-dimensional thermal conduction. Later, Luikov et al. [2] presented an analytical but complex solution for the semi-infinite plate using a generalized Fourier sine transform. However, no numerical results were reported in [2]. The case of a finite plate was analysed in [3] by expanding the interfacial temperature as a power series in the square root of distance along the plate. An approximate solution of the semi-infinite plate was presented by Luikov [4] assuming that the temperature in the plate varies linearly with the normal distance from the fluid–solid interface. Chida and Kato [5, 6] solved the problem by vectorial dimensional analysis. Payvar [7], Karvinen [8] and Gosse [9] extended and improved the results obtained in [2,4]. Sparrow and Chyu [10] studied the conjugate heat transfer from a vertical plate fin to a laminar forced convection flow. One-dimensional conduction equation for the fin and boundary layer equations for the fluid were solved simultaneously considering the continuity of temperature and heat flux at the solid–fluid interface. The analysis of the conjugate forced convection heat transfer from small isothermal heat sources embedded in a large substrate for hydrodynamically fully developed laminar channel flow was performed in [11].

Other solutions of the conjugate heat/mass transfer from a finite/infinite flat plate were obtained analytically or numerically in [12–31] (in agreement with the aims of this work, we restricted the citation only to the forced convection analysis in laminar flow). The following observations can be made from the analysis of the mathematical models used in [1–31]:

- the boundary layer approximation was widely used to model the transfer in the fluid;
- except for Pozzi and coworkers [12,16,24,25,28] (and the references cited herein), Dorfman [27] and Juncu [29], a steady temperature profile in both phases was assumed; Pozzi and co-workers, focused on the unsteady conjugate heat transfer problem from a semi-infinite plate; an integral formulation of the boundary layer equations models the heat transfer in the fluid phase; in the solid, the heat

* Tel.: +40 21 345 0596; fax: +40 21 345 0596.
E-mail address: juncu@easynet.ro.

1290-0729/$ – see front matter
doi:10.1016/j.ijthermalsci.2007.09.002

Nomenclature

c_P	heat capacity
k	thermal conductivity
L	plate length
Nu	Nusselt number
Pr	Prandtl (Schmidt) number, $Pr = \nu/\alpha_f$
Re	Reynolds number based on plate length, $Re = U_\infty L/\nu$
t	time
T	temperature
x	streamwise (horizontal) coordinate
X	nondimensional streamwise coordinate, $X = x/L$
y	transverse (vertical) coordinate
Y	nondimensional transverse coordinate, $Y = y/L$
Z	dimensionless temperature defined by the relation, $Z_{f(p)} = \frac{T_{f(p)} - T_{f,\infty}}{T_{p,0} - T_{f,\infty}}$

Greek symbols

α	thermal diffusivity
ε	aspect ratio
Φ	conductivity ratio, k_p/k_f
ν	kinematic viscosity of the fluid phase
ρ	density
τ	dimensionless time or Fourier number, $\tau = t\alpha/L^2$
ω	dimensionless vorticity
ψ	dimensionless stream function
Ξ	volume heat capacity ratio, $(\rho_p c_{P,p})/(\rho_f c_{P,f})$

Subscripts

ext	refers to external value
f	refers to the fluid
int	refers to internal value
p	refers to plate
0	initial conditions
∞	large distance from the plate

transfer in the axial direction is neglected (one dimensional, linear variation in the direction normal to interface); in [27] the one dimensional transient conduction equations for the wet and dry portions of the plate, conjugated at the moving film front, were solved; the unsteady forced convection heat transfer from a finite plate with spatially uniform temperature was analysed numerically in [29].

To our knowledge, the only fully numerical solution of the conjugate problem was obtained in [22]. Considering the temperature of the unwetted side of the plate constant, Vynnycky et al. [22] presented steady numerical solutions for $10^2 \leqslant Re \leqslant 10^4$, $Pr = 10^{-2}$, 1, 10^2, $\varepsilon = 0.25$, 1 and $\Phi = 1, 2, 5$ and 20.

A steady temperature profile inside the plate and in the fluid phase can be achieved only if a heat/mass source is present in the system. When there is no heat/mass source in the system, the conjugate problem must be rewritten and solved as an unsteady one. The aim of this paper is to analyse the unsteady conjugate heat/mass transfer from a flat plate. To our knowledge, this problem was not investigated until now. The influence of the physical properties ratio and aspect ratio on the heat/mass transfer rate is investigated for $Re = 100$ (Re is the plate Reynolds number) and for three values of the Prandtl number, $Pr = 0.1$, 1 and 10.

2. Model equations

Consider the steady, laminar, incompressible, two dimensional motion of a Newtonian fluid at zero incidence past a hot or cold flat plate occupying the region $-L/2 \leqslant x \leqslant L/2$, $-\varepsilon L \leqslant y \leqslant 0$ (see Fig. 1). The plate has finite length L and thickness εL. The ambient forced flow occupies the region, $-\infty < x < \infty$, $y \geqslant 0$ (the same situation as in [22]). The free stream velocity and concentration/temperature are denoted by U_∞ and C_∞/T_∞, respectively. The sides of the plate located

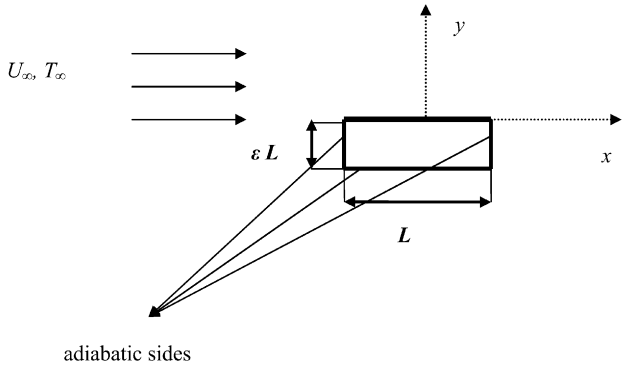

Fig. 1. Schematic of the problem.

at $y = -\varepsilon L$ and $x = \pm(L/2)$ are insulated. Due to the complexities of the problem, we consider also valid the following statements:

- the effects of buoyancy and viscous dissipation are negligible;
- the physical properties of the material of the plate and the fluid are considered to be uniform, isotropic and constant;
- no emission or absorption of radiant energy;
- no phase change;
- no chemical reaction inside the plate or in the surrounding fluid;
- no pressure diffusion or thermal diffusion.

The assumptions practiced in this work are those usually employed in the analysis of the analogy between heat and mass transfer. For the simplicity and clarity of the presentation, in the remainder of this work, we will use only the terminology specific to heat transfer. This does not mean however that the implication of the present results in mass transfer should be ignored.

Nondimensionalizing the basic conservation balances for momentum and thermal energy using the free stream fluid properties and the plate length, we obtain the governing differential equations:

– fluid motion

$$\frac{\partial^2\psi}{\partial X^2}+\frac{\partial^2\psi}{\partial Y^2}=\omega,\quad -\infty<X<\infty,\ Y>0 \tag{1a}$$

$$Re\left(\frac{\partial\psi}{\partial Y}\frac{\partial\omega}{\partial X}-\frac{\partial\psi}{\partial X}\frac{\partial\omega}{\partial Y}\right)=\frac{\partial^2\omega}{\partial X^2}+\frac{\partial^2\omega}{\partial Y^2}$$
$$-\infty<X<\infty,\ Y>0 \tag{1b}$$

– energy

$$\frac{\partial Z_f}{\partial\tau_f}+Re\,Pr\left(\frac{\partial\psi}{\partial Y}\frac{\partial Z_f}{\partial X}-\frac{\partial\psi}{\partial X}\frac{\partial Z_f}{\partial Y}\right)$$
$$=\frac{\partial^2 Z_f}{\partial X^2}+\frac{\partial^2 Z_f}{\partial Y^2},\quad -\infty<X<\infty,\ Y>0 \tag{2a}$$

$$\frac{\partial Z_p}{\partial\tau_p}=\frac{\partial^2 Z_p}{\partial X^2}+\frac{\partial^2 Z_p}{\partial Y^2}$$
$$-1/2<X<1/2,\ -\varepsilon<Y<0 \tag{2b}$$

in which

$$Re=\frac{U_\infty L}{\nu},\qquad Pr=\frac{\nu}{\alpha}$$

The boundary conditions are:

$$\psi=\omega=\frac{\partial Z_f}{\partial Y}=0,\quad |X|>1/2,\ Y=0 \tag{3a}$$

$$\psi=\frac{\partial\psi}{\partial Y}=0,\qquad Z_f=Z_p$$

$$\Phi\frac{\partial Z_p}{\partial Y}=\frac{\partial Z_f}{\partial Y},\quad |X|\leqslant 1/2,\ Y=0 \tag{3b}$$

$$\frac{\partial Z_p}{\partial X}=0,\quad X=\pm\frac{1}{2},\ -\varepsilon\leqslant Y\leqslant 0 \tag{3c}$$

$$\frac{\partial Z_p}{\partial Y}=0,\quad |X|\leqslant\frac{1}{2},\ Y=-\varepsilon \tag{3d}$$

$$\psi\to Y,\qquad \omega\to 0,\qquad Z_f\to 0$$
$$r=(X^2+Y^2)^{1/2}\to\infty \tag{3e}$$

The dimensionless initial conditions are:

$$\tau=0,\qquad Z_p=1$$
$$Z_f\big(|X|>1/2, Y\geqslant 0\quad\text{and}\quad |X|\leqslant 1/2, Y>0\big)=0 \tag{4}$$

The physical quantities of interest are the plate average temperature $\bar{Z}_p$, the local Nusselt number, Nu_X, the overall Nusselt number, $Nu_{p(f)}$ and the fractional Nusselt numbers, Nu_{int}, Nu_{ext}. Considering as driving force the difference between the instantaneous plate average temperature and the free stream temperature, the local and overall Nu numbers (Nu_p if $\Phi\leqslant 1$ and Nu_f if $\Phi>1$) are given by

$$Nu_X=-\frac{1}{\bar{Z}_p}\frac{\partial Z_f}{\partial Y}\bigg|_{Y=0} \tag{5}$$

$$Nu_{f(p)}=-(\Phi)\frac{1}{\bar{Z}_p}\int_{-1/2}^{1/2}\frac{\partial Z_f}{\partial Y}\bigg|_{Y=0}\mathrm{d}X \tag{6a}$$

or

$$Nu_{p(f)}=-\varepsilon(\Xi)\frac{\mathrm{d}\ln\bar{Z}_p}{\mathrm{d}\tau_p} \tag{6b}$$

The plate average temperature was calculated with the relation

$$\bar{Z}_p=\frac{1}{\varepsilon}\int_{-\varepsilon}^{0}\int_{-1/2}^{1/2}Z_p\,\mathrm{d}X\,\mathrm{d}Y \tag{7}$$

The fractional Nusselt numbers were computed as

$$Nu_{\text{int}}=-\frac{1}{\bar{Z}_p-\bar{Z}_{p,s}}\int_{-1/2}^{1/2}\frac{\partial Z_f}{\partial Y}\bigg|_{Y=0}\mathrm{d}X \tag{8a}$$

$$Nu_{\text{ext}}=-\frac{1}{\bar{Z}_{p,s}}\int_{-1/2}^{1/2}\frac{\partial Z_f}{\partial Y}\bigg|_{Y=0}\mathrm{d}X \tag{8b}$$

where $\bar{Z}_{p,s}$ is the dimensionless surface average temperature of the plate,

$$\bar{Z}_{p,s}=\int_{-1/2}^{1/2}Z_p|_{Y=0}\,\mathrm{d}X \tag{9}$$

The relation between the fractional and overall Nu numbers is

$$\frac{1}{Nu_p}=\frac{1}{Nu_{\text{int}}}+\Phi\frac{1}{Nu_{\text{ext}}}\quad\text{if }\Phi\leqslant 1$$
$$\frac{1}{Nu_f}=\frac{1}{\Phi}\frac{1}{Nu_{\text{int}}}+\frac{1}{Nu_{\text{ext}}}\quad\text{if }\Phi\geqslant 1$$

3. Method of solution

The energy balance equations and the Navier–Stokes equations were solved numerically. The finite difference method was used for discretization.

The Navier–Stokes equations being uncoupled from the energy balance equations can be solved independently of them. The algorithm employed is the nested defect-correction iteration [32,33]. Eq. (1a) was discretized with the central second order accurate finite difference scheme. A double discretization (upwind and central finite difference schemes), necessary for the defect correction iteration, was used for Eq. (1b). Numerical experiments were made with the discretization steps $\Delta X=\Delta Y=1/64, 1/128, 1/256$.

The main problem in solving numerically the present Navier–Stokes equations is the boundary conditions at infinity. The simplest and most common approach is simply to use the uniform stream condition (3e) at large but finite values of X and Y, denoted as X_∞ and Y_∞. The numerical experiments made in [34] showed that this method provides accurate results when $Gr\geqslant 0$ (Gr is the Grashof number for heat transfer—in

Table 1
Asymptotic values of the overall and fractional *Nu* numbers for $Re = 100$, $Pr = 1$ and $\varepsilon = 1$

Φ	Ξ								
	0.01	0.1	0.2	0.5	1	2	5	10	100
0					2.4674				
0.01	2.46[a]	2.46	2.46	2.46	2.46	2.461	2.46	2.46	2.46
	2.469[b]	2.469	2.469	2.469	2.469	2.469	2.469	2.469	2.469
	7.38[c]	7.486	7.492	7.495	7.495	7.495	7.495	7.495	7.495
0.1	2.39	2.402	2.403	2.403	2.403	2.403	2.403	2.403	2.403
	2.485	2.483	2.483	2.483	2.483	2.483	2.483	2.483	2.483
	6.32	7.37	7.43	7.47	7.48	7.48	7.49	7.49	7.49
0.2	2.28	2.337	2.339	2.34	2.34	2.34	2.34	2.34	2.34
	2.498	2.498	2.497	2.497	2.497	2.497	2.497	2.497	2.497
	5.20	7.25	7.37	7.43	7.46	7.47	7.48	7.48	7.48
0.5	1.795	2.15	2.16	2.164	2.167	2.167	2.167	2.168	2.168
	2.624	2.542	2.54	2.538	2.538	2.538	2.537	2.537	2.537
	2.84	6.92	7.19	7.35	7.40	7.43	7.44	7.45	7.46
1	1.063	1.859	1.89	1.91	1.916	1.919	1.92	1.92	1.92
	2.785	2.608	2.601	2.596	2.595	2.595	2.594	2.594	2.594
	1.72	6.47	6.94	7.22	7.32	7.37	7.40	7.41	7.42
2	1.061	2.814	2.96	3.05	3.07	3.09	3.09	3.10	3.10
	2.896	2.708	2.692	2.683	2.680	2.678	2.678	2.677	2.677
	1.30	5.86	6.58	7.04	7.20	7.28	7.33	7.34	7.35
5	1.015	3.77	4.256	4.57	4.68	4.73	4.765	4.776	4.786
	2.960	2.850	2.827	2.813	2.809	2.807	2.805	2.804	2.804
	1.09	5.13	6.09	6.77	7.02	7.14	7.21	7.24	7.26
10	0.986	4.12	4.854	5.38	5.569	5.666	5.723	5.743	5.76
	2.980	2.920	2.90	2.890	2.890	2.885	2.884	2.884	2.883
	1.02	4.80	5.83	6.61	6.898	7.05	7.14	7.17	7.20
100	0.967	4.385	5.43	6.26	6.59	6.77	6.878	6.916	6.945
	2.99	2.99	2.99	2.99	2.99	2.99	2.985	2.985	2.985
	0.97	4.45	5.53	6.40	6.74	6.93	7.04	7.08	7.11
∞	0.92	4.56	5.68	6.59	6.95	7.13	7.25	7.29	7.32

[a] Overall *Nu* number, Nu_p if $\Phi < 1$, Nu_f if $\Phi \geqslant 1$. [b] Internal *Nu* number, Nu_{int}. [c] External *Nu* number, Nu_{ext}.

[34] a combined forced and free convection flow was studied). The method was found to be entirely unsatisfactory for $Gr < 0$. To solve the case $Gr < 0$, Robertson et al. [34] used the so-called far-field corrections for both ψ and ω. For a similar flow problem (without natural convection), Leal [35] did not find necessary the far-field corrections. However, Leal [35] recommended a carefully evaluation of the influence of ∞ on the solutions. In spite of these facts, far-field corrections similar to those proposed in [34] were used in [22], in the absence of any free convection phenomena.

Some ideas in solving the steady, laminar flow past a finite flat plate were lent from the steady, laminar flow past a circular cylinder. A reference study in this field may be considered [36]. According to [36], at X_∞ and Y_∞, the boundary conditions

$$\frac{\partial \hat{\psi}}{\partial X(Y)} = \frac{\partial \omega}{\partial X(Y)} = 0 \tag{10}$$

provide accurate results at moderate *Re* values. In (10), $\hat{\psi} = \psi - Y$ is the deviation from the uniform flow.

Numerical experiments were made with both relations (3e) and (10) as boundary conditions at infinity. The velocity profiles used in the computations of the conjugate heat transfer were calculated by solving numerically the Navier–Stokes equations with boundary conditions (10) at infinity.

The spatial derivatives of Eq. (2a) were discretized with the exponentially fitted scheme [37]. The standard central order scheme was used to approximate numerically the spatial derivatives of (2b). The discretization steps in both spatial directions are equal and took the values 1/64, 1/128 and 1/256. The discrete parabolic equation was solved by the implicit ADI method. The time step was variable and changed from the start of the computation to the final stage. The initial and final values of the time step depend on the parameter values.

4. Results

The flat plate was the first case for which the problem of conjugate transfer was formulated. However, the flat plate is not the single geometry for which the problem of conjugate transfer was solved, [38] (for the unsteady conjugate heat/mass transfer from an infinite cylinder) and [39,40] (for the unsteady conjugate heat/mass transfer from a sphere).

The infinite cylinder and the sphere are bodies characterized by a single geometric quantity. The influence of this geometric quantity on the conjugate heat transfer is quantified by the dimensionless groups, Reynolds or Peclet. The finite plate is characterized by two geometric quantities: length and thickness. The finite plate dimensionless groups are defined based on the plate's length. Thus, in comparison with the infinite cylinder and the sphere, the finite plate exhibits a new parameter, the

Table 2
Asymptotic values of the overall and fractional *Nu* numbers at $Re = 100$, $Pr = 0.1$ and $\varepsilon = 1$

Φ	Ξ								
	0.01	0.1	0.2	0.5	1	2	5	10	100
0					2.4674				
0.01	2.45[a]	2.45	2.45	2.45	2.45	2.45	2.45	2.45	2.45
	2.47[b]	2.47	2.47	2.47	2.47	2.47	2.47	2.47	2.47
	2.81[c]	3.13	3.15	3.16	3.165	3.17	3.17	3.17	3.17
0.1	1.50*	2.305	2.31	2.31	2.315	2.32	2.32	2.32	2.32
	2.67*	2.51	2.50	2.50	2.50	2.50	2.50	2.50	2.50
	0.345*	2.82	2.99	3.10	3.13	3.15	3.16	3.16	3.16
0.2	0.71*	2.12	2.15	2.17	2.17	2.18	2.18	2.18	2.18
	2.84*	2.55	2.54	2.536	2.53	2.53	2.53	2.53	2.53
	0.19*	2.50	2.83	3.00	3.05	3.12	3.14	3.15	3.15
0.5	0.27*	1.55	1.72	1.80	1.82	1.83	1.835	1.84	1.84
	2.94*	2.68	2.64	2.62	2.615	2.61	2.61	2.61	2.61
	0.14*	1.83	2.45	2.86	2.99	3.05	3.09	3.10	3.12
1	0.12*	0.93	1.18	1.35	1.40	1.42	1.43	1.44	1.44
	2.97*	2.81	2.75	2.72	2.71	2.70	2.70	2.70	2.69
	0.11*	1.39	2.08	2.66	2.88	2.98	3.05	3.08	3.10
2	0.11*	0.98*	1.39	1.74	1.86	1.92	1.96	1.97	1.98
	2.99*	2.90	2.86	2.82	2.81	2.80	2.80	2.80	2.79
	0.11*	1.18*	1.84	2.51	2.79	2.93	3.02	3.06	3.07
5	0.1*	0.97*	1.48	2.02	2.26	2.40	2.47	2.50	2.51
	2.99*	2.96	2.94	2.92	2.91	2.90	2.90	2.90	2.89
	0.1*	1.04*	1.65	2.35	2.68	2.87	2.98	3.02	3.04
10	0.09*	0.95*	1.49	2.08	2.41	2.57	2.69	2.73	2.75
	2.99*	2.98	2.97	2.96	2.95	2.95	2.95	2.94	2.94
	0.09*	0.98*	1.57	2.23	2.63	2.83	2.96	3.00	3.03
100	0.08*	0.95	1.50	2.20	2.56	2.78	2.91	2.96	3.01
	2.99*	2.99	2.99	2.99	2.99	2.99	2.99	2.99	2.99
	0.08*	0.95	1.51	2.22	2.58	2.80	2.94	2.99	3.04
∞	0.12	0.97	1.54	2.27	2.66	2.89	3.04	3.09	3.13

* Unfrozen asymptotic value. [a] Overall *Nu* number, Nu_p if $\Phi < 1$, Nu_f if $\Phi \geqslant 1$. [b] Internal *Nu* number, Nu_{int}. [c] External *Nu* number, Nu_{ext}.

dimensionless thickness ε. The analysis made in [29] reveals that, for the external problem, the asymptotic values of the *Nu* number depends on the product $\varepsilon\Xi$. Solving the internal problem (i.e. Eq. (2b) with the boundary conditions (3c), (3d) and $Z_p = 0$ at $Y = 0$ and the initial condition (4)) we found that the product (asymptotic value of *Nu*) $\times$ (ε) is a constant that does not depend on ε. Under these conditions, the following problem occurs: for given *Re* and *Pr* values, does the unsteady conjugate heat transfer from a flat plate depend explicitly on ε? Or, perhaps, the influence of the aspect ratio can be expressed by means of different parameters combinations? In this work we tried to find an answer to this problem.

We considered a single *Re* number value, $Re = 100$. The forced convection heat transfer from a flat plate is usually studied for three distinct sets of *Pr* values, e.g. $Pr \ll 1$, $Pr \approx 1$ and $Pr \gg 1$. In this work, *Pr* takes the following three values, $Pr = 0.1$, $Pr = 1$ and $Pr = 10$. For small values of the Peclet number, i.e. the product *Re Pr*, the behaviour of the system approaches that of the motionless systems. For motionless systems, in conjugate heat transfer, $Nu \to 0$ when $\tau \to \infty$. For very large values of the Peclet number, the numerical errors increase. For these reasons, we selected a single *Re* value, i.e. $Re = 100$, and $Pr = 0.1$, 1, 10.

The conductivity ratio, Φ and the volume capacity ratio, Ξ, take values in the range 10^{-2}–10^{2}. The values considered for the aspect ratio, ε, are: $\varepsilon = 2^w$, $w = -4$, -3, -2, -1, 0, 1, 2, 3. We considered $\varepsilon = 1$ as basic case. The other values of the aspect ratio were selected in order to investigate its influence on the heat transfer rate for a variation of approximately ± 1 order of magnitude.

The accuracy of the numerical solving of the Navier–Stokes equations is analysed in terms of the drag coefficient, C_D. For $Re = 100$, in elliptic coordinate system, Robertson et al. [34] obtained $C_D = 0.186$ ($X_\infty = 2.5$). In the Cartesian coordinate system, Vynnycky et al. [22] obtained $C_D = 0.166$ (for $X_\infty = Y_\infty = 5$). The present numerical experiments show that for $X_\infty = Y_\infty \geqslant 4$ and boundary conditions (10) the numerical values of the drag coefficient remain practically constant. The value obtained for C_D is $C_D = 0.171$. We observe that this value does not coincide with that calculated in [29] in elliptic coordinate system, i.e. $C_D = 0.18$. In all our numerical experiments, even using a local mesh refinement algorithm in the vicinity of the plate, the results obtained in Cartesian coordinates do not match perfectly those obtained in elliptic coordinates. The numerical experience accumulated until now for this problem is not enough for an exact verdict. Similar situa-

Table 3
Asymptotic values of the overall and fractional *Nu* numbers at $Re = 100$, $Pr = 10$ and $\varepsilon = 1$

Φ	Ξ								
	0.01	0.1	0.2	0.5	1	2	5	10	100
0					2.4674				
0.01	2.464[a]	2.464	2.464	2.464	2.464	2.464	2.464	2.464	2.464
	2.468[b]	2.468	2.468	2.468	2.468	2.468	2.468	2.468	2.468
	16.30[c]	16.35	16.35	16.35	16.35	16.35	16.35	16.35	16.35
0.1	2.437	2.438	2.438	2.438	2.438	2.438	2.438	2.438	2.438
	2.475	2.475	2.475	2.475	2.475	2.475	2.475	2.475	2.475
	15.84	16.29	16.31	16.33	16.33	16.33	16.33	16.33	16.33
0.2	2.405	2.408	2.409	2.409	2.409	2.409	2.409	2.409	2.409
	2.48	2.48	2.48	2.48	2.48	2.48	2.48	2.48	2.48
	15.32	16.22	16.27	16.30	16.31	16.31	16.31	16.31	16.31
0.5	2.30	2.32	2.32	2.32	2.32	2.32	2.32	2.32	2.32
	2.51	2.50	2.50	2.50	2.50	2.50	2.50	2.50	2.50
	13.85	16.02	16.14	16.21	16.23	16.25	16.25	16.25	16.25
1	2.10	2.19	2.19	2.19	2.19	2.19	2.19	2.19	2.19
	2.56	2.54	2.53	2.53	2.53	2.53	2.53	2.53	2.53
	11.67	15.71	15.94	16.08	16.13	16.15	16.16	16.17	16.18
2	3.30	3.86	3.89	3.91	3.91	3.91	3.91	3.92	3.92
	2.66	2.59	2.59	2.59	2.59	2.59	2.59	2.59	2.59
	8.71	15.20	15.61	15.86	15.95	15.99	16.01	16.02	16.03
5	4.18	6.94	7.11	7.12	7.23	7.25	7.26	7.26	7.27
	2.84	2.72	2.71	2.70	2.70	2.70	2.70	2.70	2.70
	5.93	14.17	14.94	15.42	15.58	15.66	15.71	15.72	15.74
10	4.28	9.07	9.51	9.78	9.87	9.92	9.95	9.96	9.97
	2.92	2.82	2.81	2.80	2.80	2.80	2.80	2.80	2.80
	5.01	13.36	14.38	15.03	15.25	15.37	15.43	15.46	15.48
100	4.12	11.61	12.83	13.66	13.95	14.11	14.20	14.23	14.25
	2.99	2.98	2.975	2.97	2.97	2.97	2.97	2.97	2.97
	4.18	12.08	13.41	14.32	14.64	14.81	14.91	14.94	14.97
∞	4.25	13.34	14.64	15.49	15.78	15.94	16.04	16.07	16.09

[a] Overall *Nu* number, Nu_p if $\Phi < 1$, Nu_f if $\Phi \geqslant 1$. [b] Internal *Nu* number, Nu_{int}. [c] External *Nu* number, Nu_{ext}.

tions can be viewed at the other benchmark problems (cylinder, sphere).

It must be mentioned that in [29] and [34] the finite plate is submerged into the flowing fluid. The hydrodynamic force that acts on a submerged finite plate is different from that corresponding to the present case. However, in [29] and [34] the flow is considered symmetric about the x-axis. The computational domain is the upper half of the xy plane. Implicitly, the results presented in [29] and [34] are valid only for $y \geqslant 0$. Under these conditions we can compare the present drag coefficient with the drag coefficient values obtained in [29] and [34].

In literature there are no data to verify the accuracy of the unsteady conjugate heat transfer computations. The accuracy of the unsteady conjugate heat transfer computations is verified using the same rules as in [38] and [40] (i.e. when $\Phi \to 0$, the asymptotic values of *Nu* and Nu_{int} should tend to the solution of the internal problem; for $\Phi \to \infty$, the asymptotic values of *Nu* and Nu_{ext} should tend to the solution of the external problem). These aspects are discussed in the next paragraphs of this section. The conjugate heat transfer results presented in this section were obtained on a mesh with steps $\Delta X = \Delta Y = 1/256$. For $Pr = 1$ and 10, we considered $X_\infty = Y_\infty = 4$ while for $Pr = 0.1$, $X_\infty = Y_\infty = 8$.

We consider as starting point for our analysis the results obtained for $\varepsilon = 1$. For $Pr = 1, 0.1$ and 10 the asymptotic values of the average *Nu* numbers (overall and fractional) are presented in Tables 1–3 and plotted in Figs. 2, 3, respectively. For $Pr = 0.1$ and 10 we plotted in Fig. 3 only the overall *Nu* number. The graphs for Nu_{int} and Nu_{ext} are similar to Figs. 2(b) and (c) with the mention that the influence of Ξ is stronger for $Pr = 0.1$ and slower for $Pr = 10$. In each cell of Tables 1–3 the first line shows the asymptotic value of the overall *Nu* number, the second line the asymptotic value of the internal *Nu* number and the third line the asymptotic external *Nu* number. The presence of the superscript $*$ in a cell indicates that the time variation of *Nu* does not reach a frozen asymptotic value. The values depicted in this case correspond to the integration final, when the time variation of *Nu* becomes small. The first row in each table, i.e. the row corresponding to $\Phi = 0$, shows the asymptotic *Nu* values computed for the internal problem. The asymptotic *Nu* number values calculated in [29] for the external problem are presented in the last row of each table (the row corresponding to $\Phi = \infty$).

Tables 1–3 show a very good agreement between the present solutions (overall and internal *Nu* numbers) and the solution of the internal problem when $\Phi \to 0$. When $\Phi \to \infty$, the present values of the asymptotic *Nu* numbers (overall and external) tend to the solution of the external problem. As in the case of the drag coefficient, a difference between the Cartesian coordinate data and elliptic coordinate data exits. This difference increases

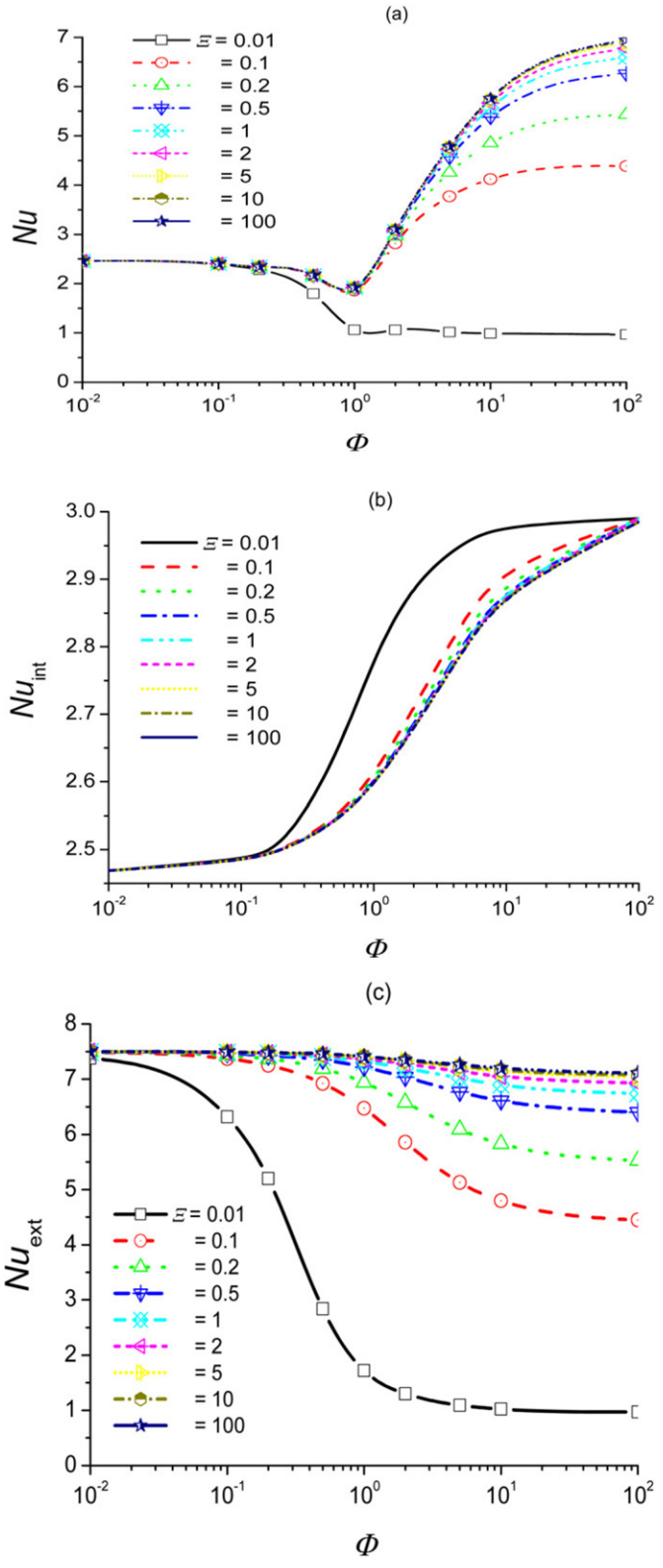

Fig. 2. The influence of the conductivity ratio (Φ) and heat capacity ratio (Ξ) on the asymptotic values of the *Nu* numbers for $Re = 100$, $Pr = 1$ and $\varepsilon = 1$; (a) overall *Nu* number; (b) internal *Nu* number; (c) external *Nu* number.

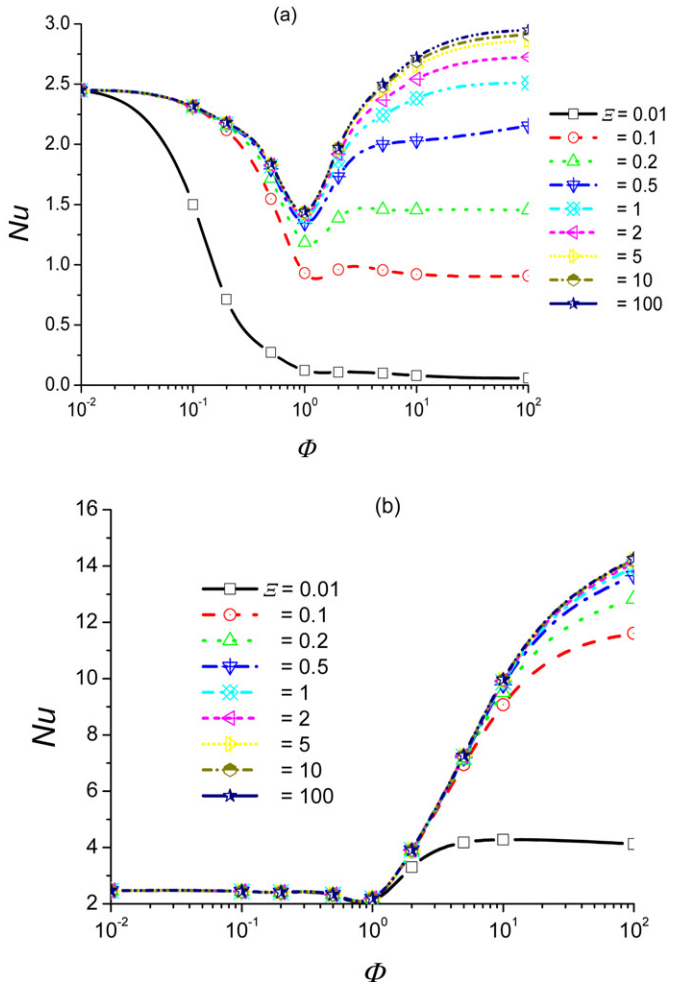

Fig. 3. The influence of the conductivity ratio (Φ) and heat capacity ratio (Ξ) on the asymptotic values of the overall *Nu* numbers for $Re = 100$ and $\varepsilon = 1$; (a) $Pr = 0.1$; (b) $Pr = 10$.

with the increase in Pr. During the present numerical experiments we observed the presence of a persistent difference, around 1.5–3%, between the asymptotic *Nu* values provided by relations (6a) and (6b). Note that for cylinder and sphere this difference is smaller than 1% and may be considered numerical error. In the case of the finite flat plate we think that this discrepancy is due to the fact that the heat flux on the surface of the plate is integrally singular at $X = \pm\frac{1}{2}$. The cylinder and the sphere do not exhibit any singularity. The results presented in Tables 1–3 were calculated with relation (6b).

We expected that for $\Phi = 100$ the temperature of the plate to be spatially uniform. The numerical simulations made show that, for $\Phi = 100$, the difference between $\bar{Z}_p$ and $\bar{Z}_{p,s}$ increases with the increase in Pr (from approximately 0.7% at $Pr = 0.1$ to approximately 5% at $Pr = 10$). We made some numerical experiments with $\Phi = 1000$. For $Pr = 0.1$ and 1 the results are practically the same. For $Pr = 10$, the relative difference between $\bar{Z}_p$ and $\bar{Z}_{p,s}$ becomes smaller than 1%.

A solid body has spatially uniform temperature during unsteady convection if

$$\frac{Nu_{\text{ext}}}{\Phi} < 0.1$$

Tables 1, 2 show that the previous condition is fulfilled for $Pr = 0.1$, 1 and $\Phi = 100$. Table 3 shows that for $Pr = 10$, the

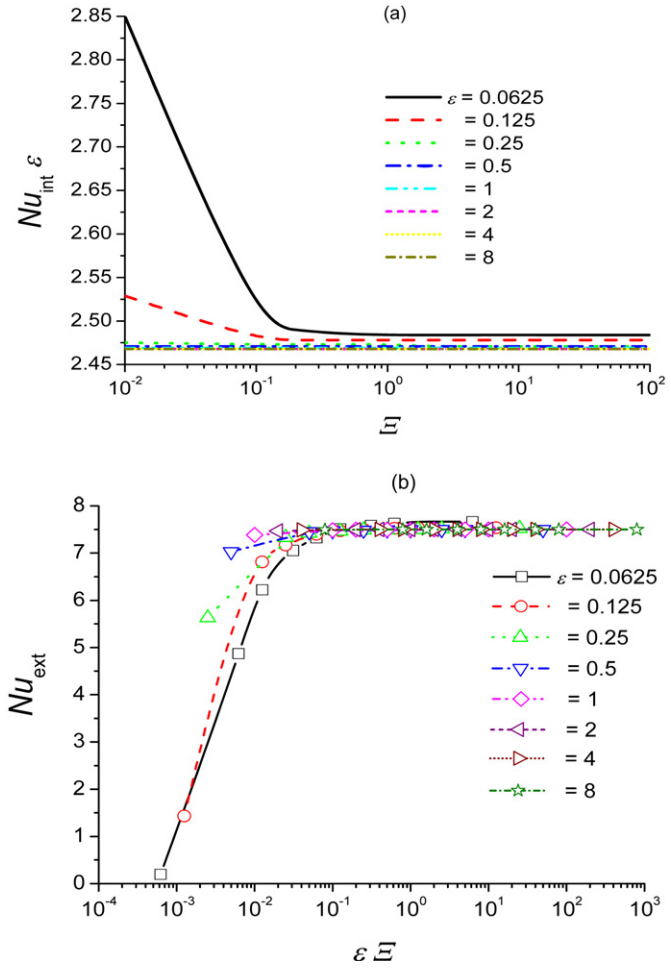

Fig. 4. The influence of the aspect ratio on the asymptotic values of the fractional *Nu* numbers for $Re = 100$, $Pr = 1$ and $\Phi = 0.01$; (a) internal *Nu* number; (b) external *Nu* number.

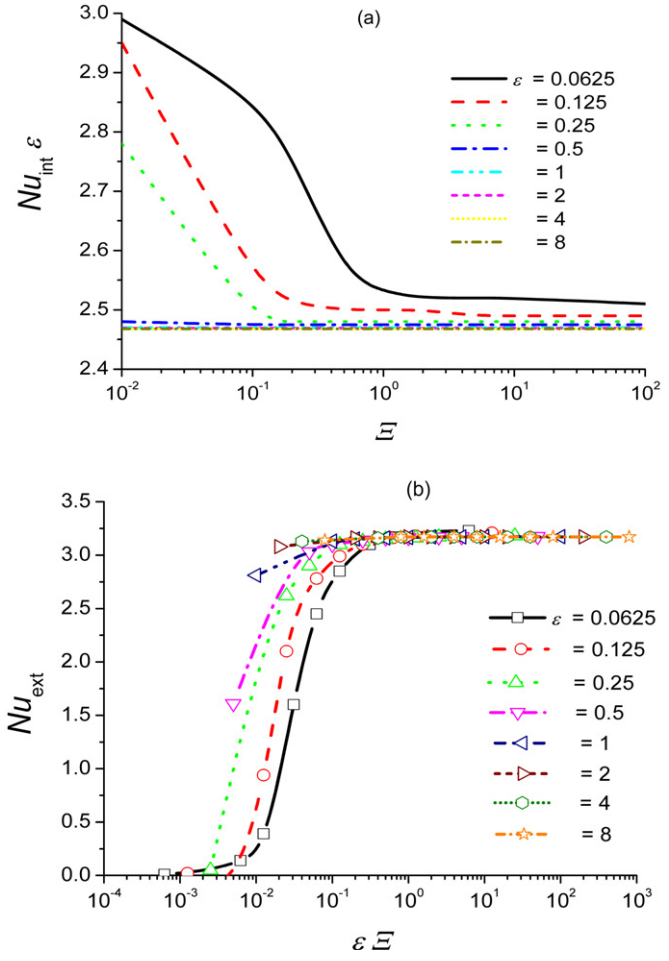

Fig. 5. The influence of the aspect ratio on the asymptotic values of the fractional *Nu* numbers for $Re = 100$, $Pr = 0.1$ and $\Phi = 0.01$; (a) internal *Nu* number; (b) external *Nu* number.

previous criterion is satisfied when $\Phi > 100$. Note that the ratio (Nu_{ext}/Φ) is also known as the Biot number.

Tables 1–3 and Figs. 2, 3 show that the influence of the conductivity ratio and heat capacity ratio on the asymptotic values of the *Nu* numbers is similar to that encountered at the cylinder [38] and the sphere [40]. However, we observe that for $\Xi \geqslant 0.1$, the data are more grouped; the influence of the heat capacity ratio on the asymptotic *Nu* numbers values is weaker. Also, the increase in *Pr* decreases the influence of Ξ. For $Pr = 1$ and 10, thermal wake [29,38,40] occurs only for $\Xi = 0.01$ and $\Phi > 0.2$ ($Pr = 1$), $\Phi > 2$ ($Pr = 10$). For $Pr = 0.1$, thermal wake occurs for $\Xi = 0.2$ and $\Phi > 2$.

The results obtained for the internal and external problems suggest the analysis of the influence of the aspect ratio on the conjugate heat transfer in terms of fractional *Nu* numbers. The following strategy was adopted in this work: for a given value of the conductivity ratio, we studied the effect of Ξ on the product (asymptotic Nu_{int}) $\times(\varepsilon)$ and the effect of the product $\varepsilon\Xi$ on the asymptotic values of Nu_{ext}. From the numerical experiments made we selected for presentation the results obtained for $\Phi = 0.01$ (Figs. 4–6), $\Phi = 1$ (Figs. 8–10) and $\Phi = 100$ (Fig. 11). The data obtained for $0.1 \leqslant \Phi \leqslant 10$ are similar to those depicted in Figs. 8–10.

For $\Phi = 0.01$ the plate controls the heat transfer. The expected results are: (1) $(Nu_{int}) \times (\varepsilon)$ constant and (2) the influence of the heat capacity ratio and aspect ratio on Nu_{ext} negligible. Figs. 4–6 show that:

(i) the influence of the aspect ratio on $(Nu_{int}) \times (\varepsilon)$ is relatively significant only for $Pr = 0.1$ and 1, small values of the heat capacity ratio ($\Xi < 1$) and small ε values ($\varepsilon < 0.125$ for $Pr = 1$ and $\varepsilon \leqslant 0.25$ for $Pr = 0.1$); in all the other situations, $(Nu_{int}) \times (\varepsilon)$ may be well approximated by the asymptotic value of the *Nu* number for the internal problem; the maximum relative difference is 2.5% (this value was obtained for $Pr = 0.1$, $\Xi \geqslant 1$, $\varepsilon = 0.0625$).

(ii) the aspect ratio influences the asymptotic Nu_{ext} values only for small values of $\varepsilon\Xi$; the $\varepsilon\Xi$ boundary value, $(\varepsilon\Xi)_{bv}$, i.e. the value for which the influence of the aspect ratio on asymptotic Nu_{ext} becomes negligible, depends on *Pr*; it varies from $(\varepsilon\Xi)_{bv} \cong 1$ at $Pr = 0.1$ to $(\varepsilon\Xi)_{bv} \cong 0.01$ at $Pr = 10$; for $\varepsilon\Xi < (\varepsilon\Xi)_{bv}$, the spread in asymptotic Nu_{ext} values is higher at small *Pr* values; we also observe that

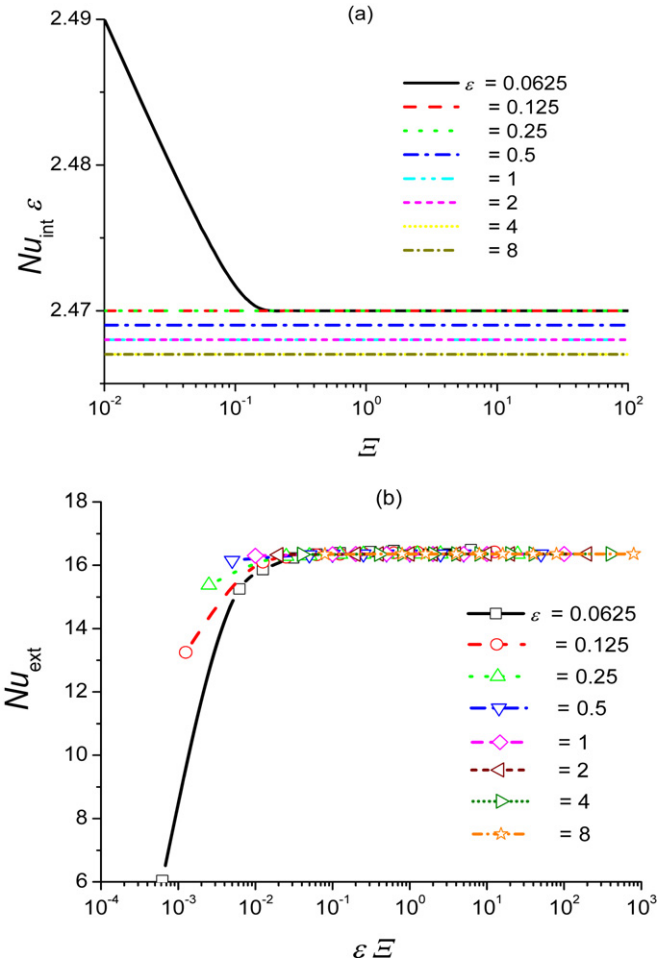

Fig. 6. The influence of the aspect ratio on the asymptotic values of the fractional *Nu* numbers for $Re = 100$, $Pr = 10$ and $\Phi = 0.01$; (a) internal *Nu* number; (b) external *Nu* number.

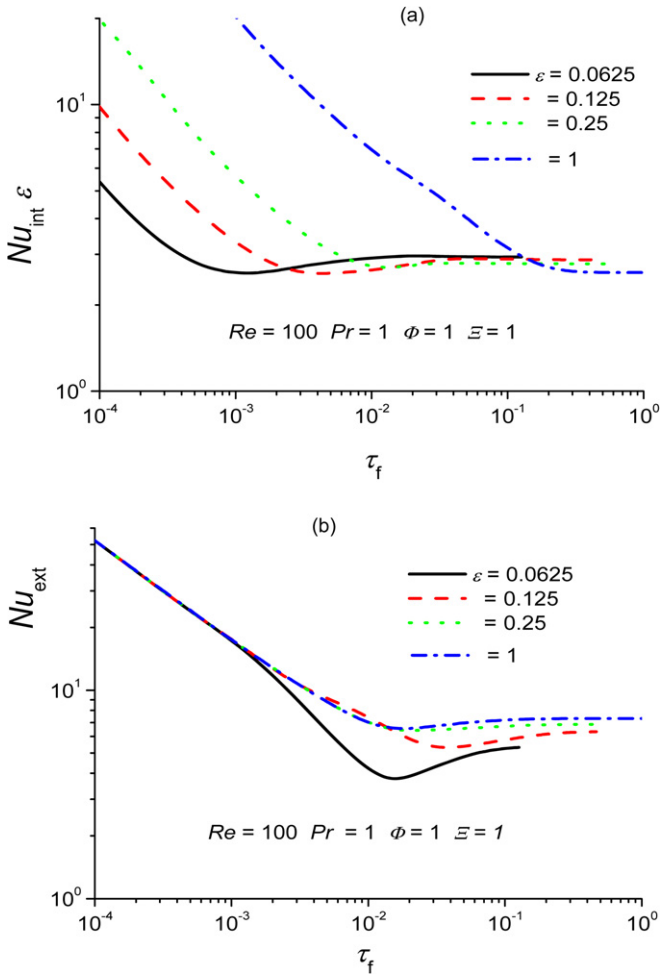

Fig. 7. Time variation of the fractional *Nu* numbers; (a) internal *Nu* number; (b) external *Nu* number.

for a given $\varepsilon\Xi$ value, $\varepsilon\Xi < (\varepsilon\Xi)_{bv}$, the decrease in ε decreases the asymptotic Nu_{ext} value.

In this moment, we should mention the following important aspect: for small values of the aspect ratio, i.e. $\varepsilon = 0.0625$ and $\varepsilon = 0.125$, the time variation of the *Nu* numbers does not stabilize; a frozen asymptotic value is not attained. The values plotted in Figs. 4–6 correspond to very small values of $\bar{Z}_p$, $10^{-4} \leqslant \bar{Z}_p \leqslant 10^{-3}$. It must be mentioned that the time integration was stopped when $\bar{Z}_p \leqslant 10^{-4}$. The previous statements are not valid only for $\Phi = 0.01$. They are valid for $\Phi < 100$ (see Fig. 7).

The present *Nu* numbers are not a direct measure of the heat transfer rate but have a nonzero asymptotic limit (for this reason they are used). They are the ratio of two instantaneous average quantities: (1) dimensionless temperature gradient on the plate surface and (2) dimensionless driving force (average plate temperature, average surface plate temperature or the difference between these two quantities). The frozen asymptotic value is reached when the temperature gradient and the driving force obey the same exponential decrease in time. For small ε values and $\Phi < 100$, the driving force decreases a bit faster than the temperature gradient. For this reason, Nu_{int} and Nu_{ext} do not reach a frozen asymptotic value.

We also made numerical experiments with $\Phi = 10^{-3}$. For $\Phi = 10^{-3}$ the influence of the aspect ratio on the asymptotic values of $(Nu_{int}) \times (\varepsilon)$ is considerably smaller. Only for $Pr = 0.1$, $\Xi = 0.01$ and $\varepsilon = 0.0625$ the asymptotic $(Nu_{int}) \times (\varepsilon)$ value is $(Nu_{int}) \times (\varepsilon) = 2.86$. In all the other cases, $(Nu_{int}) \times (\varepsilon) \cong 2.46$. For $\Phi = 10^{-3}$ the influence of the product $\varepsilon\Xi$ on the asymptotic Nu_{ext} remains significant only for $Pr = 0.1$, $\Xi = 0.01$ and $\varepsilon = 0.0625, 0.125$.

The salient features of the conjugate transfer are best emphasized by the case $\Phi = 1$. Figs. 8(a)–10(a) show that the influence of the aspect ratio on $(Nu_{int}) \times (\varepsilon)$ is simple and clear: the increase in ε decreases the asymptotic values of $(Nu_{int}) \times (\varepsilon)$. We also observe that for $\varepsilon \leqslant 0.125$ and $\varepsilon > 1$ the influence of the heat capacity ratio on $(Nu_{int}) \times (\varepsilon)$ is less significant. The influence of the aspect ratio on the asymptotic Nu_{ext} values is more complex. Figs. 8(b)–10(b) show that there exists a $\varepsilon\Xi$ value, $(\varepsilon\Xi)^*$, that separates two domains in which the influence of the aspect ratio on Nu_{ext} is different. This value depends on *Pr* and it increases with the decrease in *Pr*. Based on the previous statements, we may summarize the influence of the aspect

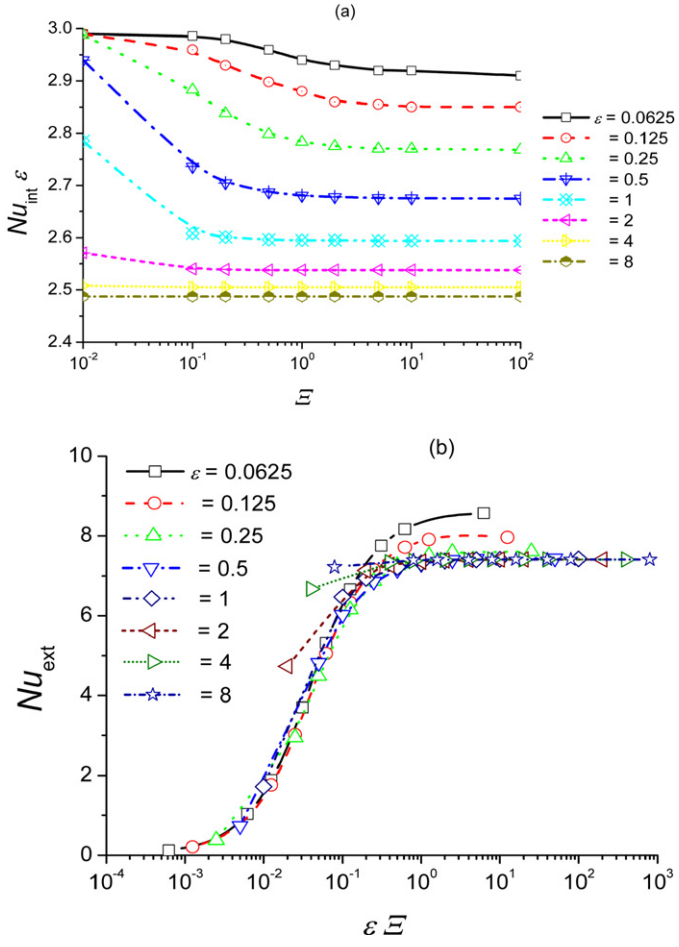

Fig. 8. The influence of the aspect ratio on the asymptotic values of the fractional *Nu* numbers for $Re = 100$, $Pr = 1$ and $\Phi = 1$; (a) internal *Nu* number; (b) external *Nu* number.

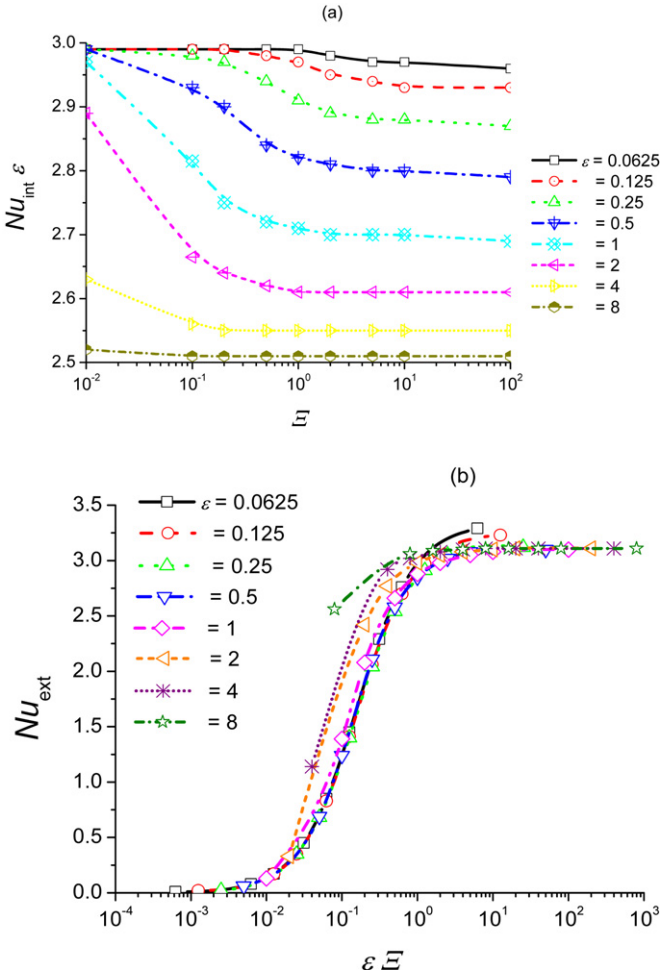

Fig. 9. The influence of the aspect ratio on the asymptotic values of the fractional *Nu* numbers for $Re = 100$, $Pr = 0.1$ and $\Phi = 1$; (a) internal *Nu* number; (b) external *Nu* number.

ratio on the asymptotic values of the external *Nu* number as follows:

- for $\varepsilon\Xi < (\varepsilon\Xi)^*$ and $\varepsilon \leqslant 1$, Nu_{ext} depends only on the product $\varepsilon\Xi$;
- for $\varepsilon\Xi < (\varepsilon\Xi)^*$ and $\varepsilon > 1$, the increase in the aspect ratio increases the asymptotic Nu_{ext} values;
- for $\varepsilon\Xi \geqslant (\varepsilon\Xi)^*$ and $\varepsilon > 0.125$, Nu_{ext} may be considered approximately constant;
- for $\varepsilon\Xi \geqslant (\varepsilon\Xi)^*$ and $\varepsilon \leqslant 0.125$, the decrease in ε increases Nu_{ext}.

For $\Phi = 100$ the behaviour of the system should be similar to that of the external problem, i.e. Nu_{ext} depends only on the product $\varepsilon\Xi$ and $(Nu_{int}) \times (\varepsilon)$ is independent from ε and Ξ. Fig. 11 shows that:

(i) the asymptotic values of Nu_{ext} depend only on the product $\varepsilon\Xi$; the influence of the aspect ratio as independent parameter may be considered negligible;
(ii) for a given value of the aspect ratio, the influence of the volume heat capacity ratio on $(Nu_{int}) \times (\varepsilon)$ is negligible; the influence of the aspect ratio on $(Nu_{int}) \times (\varepsilon)$ is relatively significant; we observe that the increase in the aspect ratio decreases the values of $(Nu_{int}) \times (\varepsilon)$; we must also mention that the increase in ε increases the difference between $\bar{Z}_p$ and $\bar{Z}_{p,s}$.

We did not plot the results obtained for $\Phi = 100$ and $Pr = 0.1$, 1 because these are similar to those plotted in Fig. 11. We must mention that the maximum relative difference between different $(Nu_{int}) \times (\varepsilon)$ values is around 1.5% (for $Pr = 0.1$) and 3% (for $Pr = 1$).

In the previous paragraphs we analysed the *local* (i.e. the analysis was made for a single value of the conductivity ratio) influence of aspect ratio on the conjugate transfer. Concerning the *global* effect of the aspect ratio on the conjugate transfer, we can make the following observation, valid only for $(Nu_{int}) \times (\varepsilon)$: for a given value of the *Pr* number, the increase in ε has approximately the same effect as the decrease in Φ. It is difficult to establish an exact relation about the conjugate action of these two parameters (especially for small values of the heat capacity ratio). However, we may approximate the conjugate action of ε and Φ by considering the ratio Φ/ε instead of Φ. For the asymptotic values of Nu_{ext} we could not find any global rule.

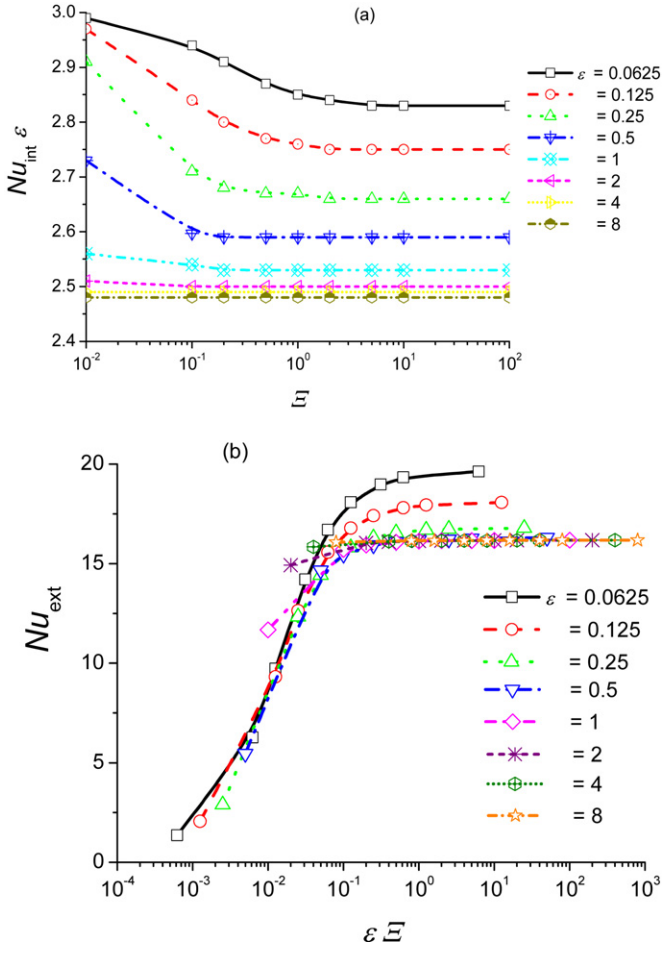

Fig. 10. The influence of the aspect ratio on the asymptotic values of the fractional *Nu* numbers for $Re = 100$, $Pr = 10$ and $\Phi = 1$; (a) internal *Nu* number; (b) external *Nu* number.

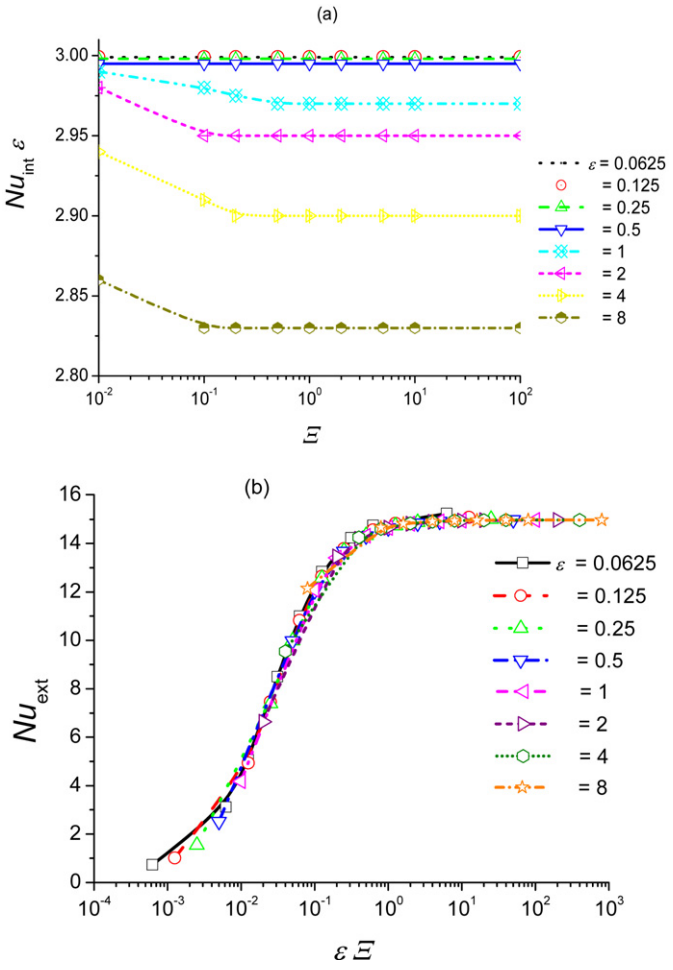

Fig. 11. The influence of the aspect ratio on the asymptotic values of the fractional *Nu* numbers for $Re = 100$, $Pr = 10$ and $\Phi = 100$; (a) internal *Nu* number; (b) external *Nu* number.

Concerning the global behaviour of the system, other observations that can be made are: the influence of the conductivity and heat capacity ratios on the conjugate heat transfer is the same for any value of the aspect ratio; the decrease in ε increases the presence of the thermal wake phenomenon.

Based on the results obtained in this section, we tried to establish some rules to estimate the asymptotic *Nu* number values without solving the heat balance equations. For other *Re*, *Pr* and ε than those used in this work, we may compute the asymptotic *Nu* values as follows:

- when $\Phi \to 0$, *Nu* tends to the solution of the internal problem; in this case, $(Nu) \times (\varepsilon) = \text{constant} \cong 2.467$; when $\Phi \to \infty$, *Nu* tends to the solution of the external problem; for given *Re* and *Pr* values, Nu_{ext} depends only on the product $\varepsilon\Xi$;
- for high values of *Re* and *Re Pr*, the influence of Ξ on asymptotic *Nu* values is negligible for $\Xi > 0.1$; for high *Re* numbers, Nu_{ext} tends to the boundary layer results, [29]; thus, for high *Re* numbers, high *Re Pr* values and $\Xi > 0.1$, the asymptotic *Nu* values may be calculated with the interpolation relation

$$\frac{1}{Nu} = \frac{1}{Nu_i} + \Phi\frac{1}{Nu_e} \quad \text{if } \Phi \leqslant 1$$

$$\frac{1}{Nu} = \frac{1}{\Phi}\frac{1}{Nu_i} + \frac{1}{Nu_e} \quad \text{if } \Phi \geqslant 1$$

where Nu_i is the asymptotic solution of the internal problem and Nu_e is the boundary layer result.

For small *Re* and *Re Pr* values it is difficult to derive any scaling law. The influence of Ξ increases with the decrease in *Re Pr*. Also for $Re\,Pr < 1$, the behaviour is similar to that of motionless systems.

The last problem discussed in this section is: for other bodies characterized by two geometric quantities, does the conjugate heat transfer follow similar or different rules? The present results were obtained under the assumption that the geometric parameter (i.e. the aspect ratio) does not affect the external flow. Thus, for similar cases (for example, the heat source embedded in a large substrate, the backward-facing step flow [41], the laminar offset jets) we think that similar results may be obtained. For bodies for which the geometric parameter influences the external flow (for example, elliptic cylinder, spheroids) it is difficult to make any prediction.

5. Conclusions

The unsteady physical conjugate heat transfer from a finite flat plate was investigated. The flow past the flat plate was considered steady, laminar at zero incidence. The plate *Re* number takes the value 100. The *Pr* number was considered equal to 0.1, 1 and 10. The main problems analysed were the influence of the physical properties ratio and the aspect ratio on the heat transfer rate.

The numerical results obtained in this work may be summarized as follows:

- for given values of the aspect ratio and *Pr* number, the influence of the conductivity and heat capacity ratios on the conjugate heat transfer is similar to that encountered at cylinder and sphere; for $\Phi \to 0$ the asymptotic *Nu* values tend to the solution of the internal problem; the solution of the internal problem does not depend on Ξ; for $\Phi \to \infty$ the asymptotic *Nu* values tend to the solutions of the external problem; the solution of the external problem depends strongly on Ξ;
- for a given *Pr* value, the quantity (asymptotic value of $Nu_{\text{int}}) \times (\varepsilon)$ may be considered dependent on Φ, ε and Ξ; for $\Phi \to 0$ (∞) the influence of Ξ and ε on (asymptotic value of $Nu_{\text{int}}) \times (\varepsilon)$ may be considered negligible;
- the influence of the aspect ratio as independent variable on the asymptotic values of external *Nu* number is relatively significant for small values of the aspect ratio ($\varepsilon \leqslant 0.125$), small values of $\varepsilon\Xi$ and $\Phi < 100$.

References

[1] Y.L. Perelman, On conjugate problems of heat transfer, Int. J. Heat Mass Transfer 3 (1961) 293–303.

[2] A.V. Luikov, V.A. Aleksashenko, A.A. Aleksashenko, Analytical methods of solution of conjugate problems in convective heat transfer, Int. J. Heat Mass Transfer 14 (1971) 1047–1056.

[3] M. Sakakibara, S. Mori, A. Tanimoto, Effect of wall conduction on convective heat transfer with laminar boundary layer, Heat Transfer Japan. Res. 2 (1973) 94–103.

[4] A.V. Luikov, Conjugate convective heat transfer problems, Int. J. Heat Mass Transfer 17 (1974) 257–265.

[5] K. Chida, Y. Katto, Study of conjugate heat transfer by vectorial dimensional analysis, Int. J. Heat Mass Transfer 19 (1976) 453–460.

[6] K. Chida, Y. Katto, Conjugate heat transfer of continuously moving surfaces, Int. J. Heat Mass Transfer 19 (1976) 461–470.

[7] P. Payvar, Convective heat transfer to laminar flow over a plate of finite thickness, Int. J. Heat Mass Transfer 20 (1977) 431–433.

[8] R. Karvinen, Some new results for conjugate heat transfer in a flat plate, Int. J. Heat Mass Transfer 21 (1978) 1261–1264.

[9] J. Gosse, Analyse simplifiée du couplage conduction–convection pour un écoulement à couche limite laminaire sur une plaque plane, Rev. Gen. Therm. 228 (1980) 967–971.

[10] E.M. Sparrow, M.K. Chyu, Conjugate forced convection–conduction analysis of heat transfer in a plate fin, J. Heat Transfer 104 (1982) 204–206.

[11] S. Ramadhyani, D.F. Moffat, F.P. Incropera, Conjugate heat transfer from small isothermal heat sources embedded in a large substrate, Int. J. Heat Mass Transfer 28 (1985) 1945–1952.

[12] A. Pozzi, M. Lupo, The coupling of conduction with forced convection over a flat plate, Int. J. Heat Mass Transfer 32 (1989) 1207–1214.

[13] S. Mori, H. Nakagawa, A. Tanimoto, M. Sakakibara, Heat and mass transfer with a boundary layer flow past a plate of finite thickness, Int. J. Heat Mass Transfer 34 (1991) 2899–2909.

[14] T.A. Rizk, C. Kleinstreuer, M.N. Özisik, Analytic solution to the conjugate heat transfer problem of flow past a heated block, Int. J. Heat Mass Transfer 35 (1992) 1519–1525.

[15] B.V.S.S.S. Prasad, S. Dey Sarkar, Conjugate laminar forced convection from a flat plate with imposed pressure gradient, J. Heat Transfer 115 (1993) 469–472.

[16] A. Pozzi, E. Bassano, L. Socio, Coupling of conduction and forced convection past an impulsively started infinite flat plate, Int. J. Heat Mass Transfer 36 (1993) 1799–1806.

[17] I. Pop, D.B. Ingham, A note on conjugate forced convection boundary-layer flow past a flat plate, Int. J. Heat Mass Transfer 36 (1993) 3873–3876.

[18] T. Liu, B.T. Campbell, J.P. Sullivan, Surface temperature of a hot film on a wall in shear flow, Int. J. Heat Mass Transfer 37 (1994) 2809–2814.

[19] R. Sugavanam, A. Ortega, C.Y. Choi, A numerical investigation of conjugate heat transfer from a flush heat source on a conductive board in laminar channel flow, Int. J. Heat Mass Transfer 38 (1995) 2969–2984.

[20] K.D. Cole, Conjugate heat transfer from a small heated strip, Int. J. Heat Mass Transfer 40 (1997) 2709–2719.

[21] C. Treviso, G. Becerra, F. Mendez, The classical problem of convective heat transfer in laminar flow over a thin finite thickness plate with uniform temperature at the lower surface, Int. J. Heat Mass Transfer 40 (1997) 3577–3580.

[22] M. Vynnycky, S. Kimura, K. Kanev, I. Pop, Forced convection heat transfer from a flat plate: the conjugate problem, Int. J. Heat Mass Transfer 41 (1998) 45–59.

[23] M. Mossad, Laminar forced convection conjugate heat transfer over a flat plate, Wärme – und Stoffübertragung (Heat Mass Transfer) 35 (1999) 371–375.

[24] A. Pozzi, R. Tognaccini, Coupling of conduction and convection past an impulsively started semi-infinite flat plate, Int. J. Heat Mass Transfer 43 (2000) 1121–1131.

[25] A. Pozzi, R. Tognaccini, Symmetrical impulsive thermo-fluid dynamic field along a thick plate, Int. J. Heat Mass Transfer 44 (2001) 3281–3293.

[26] C.F. Stein, P. Johansson, J. Bergh, L. Löfdahl, M. Sen, M. Gad-el-Hak, An analytical asymptotic solution to a conjugate heat transfer problem, Int. J. Heat Mass Transfer 45 (2002) 2485–2500.

[27] A. Dorfman, Transient heat transfer between a semi-infinite hot plate and a flowing cooling liquid film, J. Heat Transfer 126 (2004) 149–154.

[28] A. Pozzi, R. Tognaccini, Time singularities in conjugated thermo-fluid-dynamic phenomena, J. Fluid Mech. 538 (2005) 361–376.

[29] Gh. Juncu, Unsteady forced convection heat/mass transfer from a flat plate, Wärme – und Stoffübertragung (Heat Mass Transfer) 41 (2005) 1095–1102.

[30] S. Jahangeer, M.K. Ramis, G. Jilani, Conjugate heat transfer of a heat generating vertical plate, Int. J. Heat Mass Transfer 50 (2007) 85–93.

[31] M. Rebay, J. Padet, S. Kakaç, Forced convection from a microstructure on a flat plate, Wärme – und Stoffübertragung (Heat Mass Transfer) 43 (2007) 309–317.

[32] Gh. Juncu, R. Mihail, Numerical solution of the steady incompressible Navier–Stokes equations for the flow past a sphere by a multigrid defect correction technique, Int. J. Numer. Meth. Fluids 11 (1990) 379–395.

[33] Gh. Juncu, A numerical study of steady viscous flow past a fluid sphere, Int. J. Heat Fluid Flow 20 (1999) 414–421.

[34] G.E. Robertson, J.H. Seinfeld, L.G. Leal, Combined forced and free convection flow pas a horizontal flat plate, AIChE J. 19 (1973) 998–1008.

[35] L.G. Leal, Steady separated flow in a linearly decelerated free stream, J. Fluid Mech. 59 (1973) 513–535.

[36] B. Fornberg, A numerical study of steady viscous flow past a circular cylinder, J. Fluid Mech. 98 (1980) 819–855.

[37] P.W. Hemker, A numerical study of stiff two-point boundary problems, Ph.D. Thesis, Mathematisch Centrum, Amsterdam, 1977.

[38] Gh. Juncu, Unsteady conjugate heat/mass transfer from a circular cylinder in laminar crossflow at low Reynolds numbers, Int. J. Heat Mass Transfer 47 (2004) 2469–2480.

[39] H. Brauer, Instationärer Wärmetransport durch die Grenzfläche von Kugeln, Wärme – und Stoffübertragung (Heat Mass Transfer) 12 (1979) 145–156.

[40] Gh. Juncu, The influence of the Henry number on the conjugate mass transfer from a sphere: I—Physical mass transfer, Wärme – und Stoffübertragung (Heat Mass Transfer) 37 (2001) 519–530.

[41] P.R. Kanna, M.K. Das, Conjugate heat transfer study of backward-facing step flow—A benchmark problem, Int. J. Heat Mass Transfer 49 (2006) 3929–3941.